

Highly Pathogenic Avian Influenza A(H7N3) Virus in Poultry, United States, 2020

Sungsu Youk,¹ Dong-Hun Lee,¹ Mary L. Killian, Mary J. Pantin-Jackwood, David E. Swayne, Mia K. Torchetti

An outbreak of low-pathogenicity avian influenza A(H7N3) virus of North American wild bird lineage occurred on commercial turkey farms in North Carolina and South Carolina, USA, during March–April 2020. The virus mutated to the highly pathogenic form in 1 house on 1 farm via recombination with host 28S rRNA.

Highly pathogenic avian influenza viruses (HPAIVs) have devastating impacts on the poultry industries. With infections in poultry, H5 and H7 low-pathogenicity avian influenza viruses (LPAIVs) have spontaneously mutated into HPAIVs by different mechanisms, one of which is acquisition of basic amino acids at the hemagglutinin (HA) cleavage site (1).

In March 2020, an outbreak of LPAIV H7N3 occurred in turkey farms, affecting 11 premises in North Carolina and 1 in South Carolina, USA. The initial decision to depopulate LPAIV-affected flocks was based on a risk assessment that included the location of affected premises, the poultry density in the area, and the presence of a basic amino acid substitution at the cleavage site among the initial LPAIV detections (PEKPKTR/GLF; substitution sequence is underscored). During the ongoing response for this event, the Clemson Veterinary Diagnostic Center in Columbia, South Carolina, a member of the National Animal Health Laboratory Network, detected an influenza A(H7) outbreak in a second turkey location in South Carolina, with increased death and respiratory signs; oropharyngeal and cloacal swab samples were forwarded to the National Veterinary Services Laboratories in Ames, Iowa, USA. On April 8, the

National Veterinary Services Laboratories confirmed 1 of 6 pooled samples as HPAIV H7N3. Subsequent testing from all infected barns on the premises determined that HPAIV was present in only 1 of the 5 barns, but LPAIV was identified in the other 4 barns. All the premises affected by LPAIV and HPAIV H7N3 were located in 3 adjacent counties and 1 across state lines, indicating that geographic proximity was relevant to the outbreaks. Immediate depopulation was performed on the LPAIV- and HPAIV-affected premises, affecting 361,000 birds.

Complete genome sequencing and phylogenetic analyses were conducted to trace the origin and evolution of the H7N3 viruses. A total of 29 H7N3 viruses from 13 premises were sequenced (Appendix Table 1, <https://wwwnc.cdc.gov/EID/article/26/12/20-2790-App1.pdf>). Complete genome sequences have been deposited in GenBank (accession nos. MT444183–350 and MT444352–415). The intravenous pathogenicity index of selected LPAIV strains was 0 and of selected HPAIV strains, 2.46. Based on the HA cleavage site motif and supported by the intravenous pathogenicity index, 2 H7N3 viruses from 1 house in South Carolina were considered to be HPAIV. For the 2 HPAIVs, 34 (5.7%) and 1,076 (38.8%) reads had no insertion, whereas the rest of the reads were found to have an identical 27 nucleotides insertion from host cellular 28S rRNA in the cleavage site.

The presence of LPAIV and HPAIV in 1 barn at the same time suggests that the mutation was caught early. The 27-nt insertion coding for 9 amino acids at the HA cleavage site (PENPKTDRKSRHRRIR/GLF; insertion sequence is underscored) is identical to that found in a 2017 HPAIV H7N9 from a poultry outbreak that occurred in Tennessee (2). The potential role of a palindromic sequence was suggested to be a cause of RNA recombination with host 28S rRNA (3), and similar structure is often observed among the

Author affiliations: Southeast Poultry Research Laboratory, US Department of Agriculture Agricultural Research Service, Athens, Georgia, USA (S. Youk, M. Pantin-Jackwood, D. Swayne); University of Connecticut, Storrs, Connecticut, USA (D.-H. Lee); US Department of Agriculture, Ames, Iowa, USA (M. Killian, M. Torchetti)

DOI: <https://doi.org/10.3201/eid2612.202790>

¹These authors contributed equally to this article.

H7 subtype (4); however, the exact mechanism of recombination for this particular insert remains to be elucidated. Another notable change was a 66-nt deletion in the NA stalk region from 2 premises in North Carolina. The NA stalk deletions are commonly associated with adaptation of wild bird avian influenza viruses to gallinaceous poultry (5); for these isolates, all reads had the same 66-nt deletion (e.g., no mixed population was detected). No significant amino acid change indicating adaptation to mammalian hosts was identified by using the Influenza Research Database (Appendix Table 2).

Maximum-likelihood and Bayesian relaxed clock phylogenies of each gene were generated (6,7). All phylogenies indicate that the North Carolina and South Carolina H7N3 viruses were genetically distinct from recent Mexico H7N3 HPAIV, 2016 Indiana H7N8, and 2017 Tennessee H7N9 poultry outbreak strains (Appendix Figures 1, 2) (2,8,9). All H7N3 viruses from North Carolina and South Carolina clustered together in phylogenies across all 8 gene segments and showed high levels of nucleotide identity (>99.28%). These data support a single source of LPAIV H7N3 being introduced to turkey farms in North Carolina, spreading laterally to other turkey premises, and mutating once to HPAIV during repli-

cation in turkeys from a single barn on a turkey premises in South Carolina, with no further reassortment with any other influenza strains. Furthermore, the H7 HA genes of recent US poultry events (2016, 2017, and 2020) originated from the same North American wild bird H7 clade. With several recent incursions, this H7 HA clade represents a repetitive threat to domestic poultry and carries with it the potential to mutate to HPAIV.

To increase phylogenetic resolution, nucleotide sequences from the entire protein coding regions of each virus were concatenated, with 2 modifications: the insertion at the HA cleavage site for the HPAIV was excluded, and the deletion at the NA stalk region for the 2 LPAIVs was removed. The concatenated sequences were then analyzed with Bayesian and median-joining network phylogenetic analysis (7,10). This analysis highlights that the LPAIV H7N3 diverged early into 3 well-supported genetic clusters (A, B, and C) with high posterior probabilities (posterior probability [PP] >0.99) (Figure 1). Cluster A was detected most frequently from 10 premises in both North Carolina and South Carolina and mutated to HPAIV in a single turkey location in South Carolina (Figure 2). The estimated mean time to most recent common ancestor (tMRCA) of the concatenated whole genome of

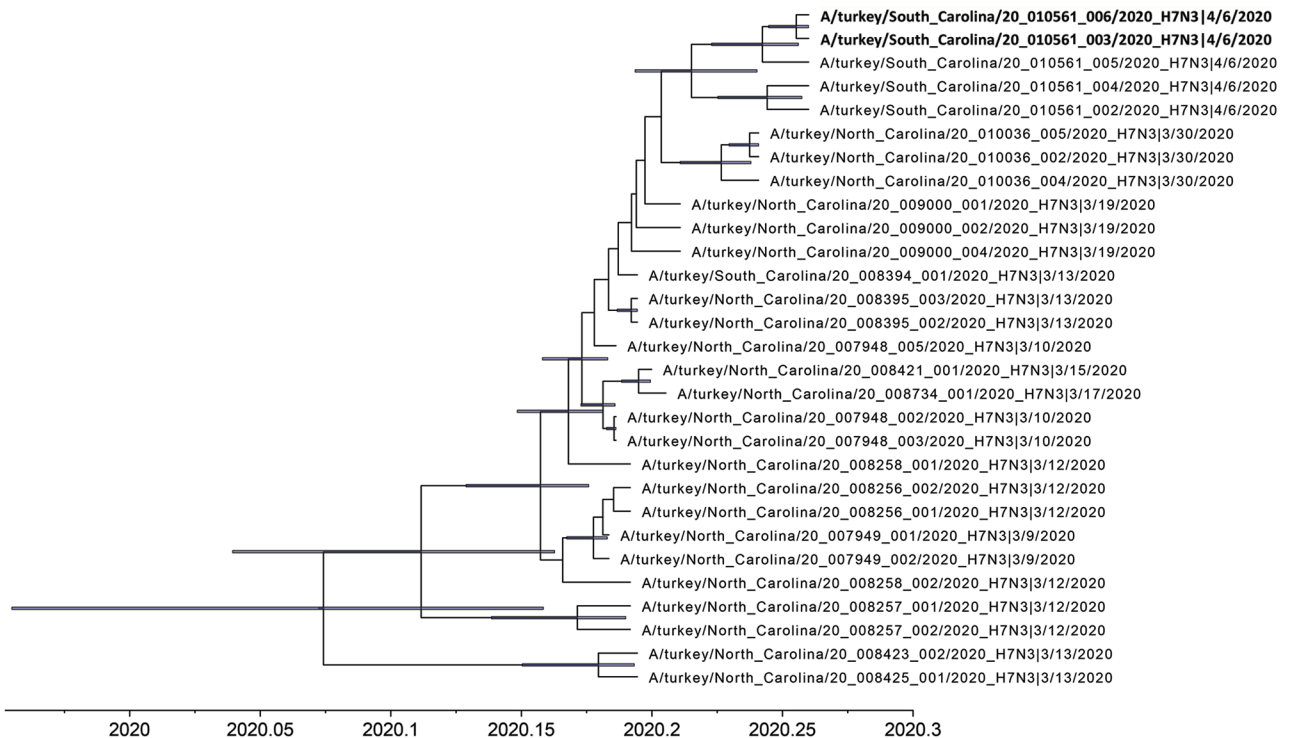


Figure 1. Time-scaled Bayesian maximum clade credibility tree of the concatenated whole genome of highly pathogenic avian influenza A(H7N3) viruses from South Carolina (bold) and North Carolina, USA. Node bars represent 95% Bayesian credible intervals for estimates of common ancestry.

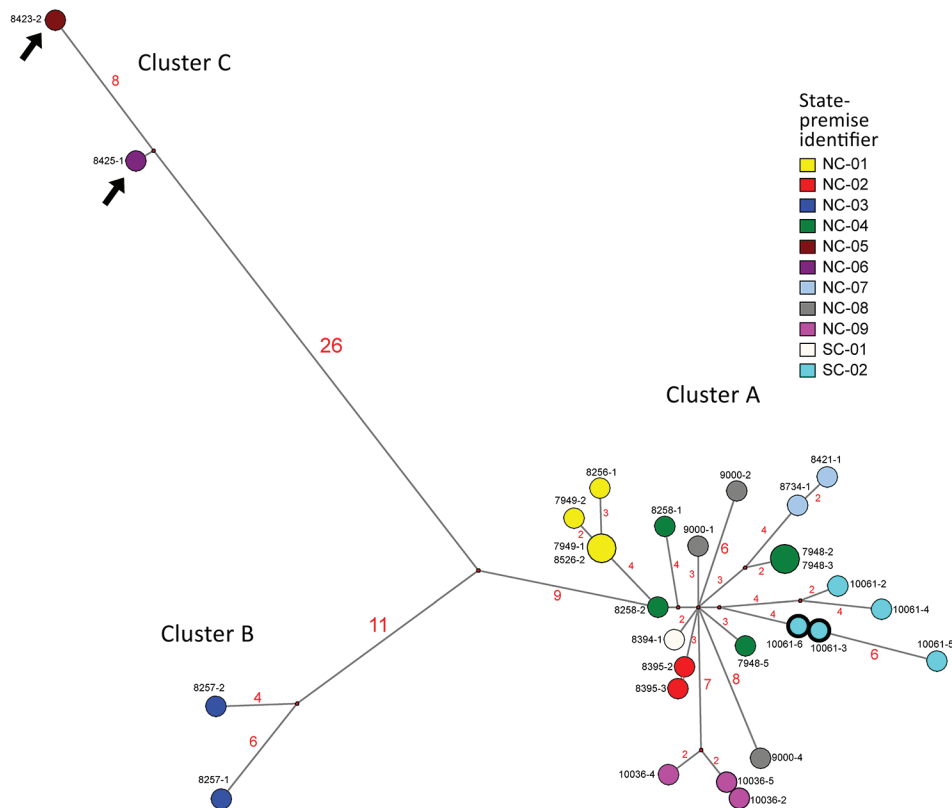


Figure 2. Median-joining phylogenetic network of the concatenated whole genome of highly pathogenic avian influenza (HPAIV) A(H7N3) viruses from South Carolina and North Carolina, USA. This network tree includes all the most parsimonious trees linking the sequences. Each unique sequence is represented by a circle sized relative to its frequency. The number of nucleotide differences between viruses is indicated on the branches. Isolates are colored according to the source premises. The black arrows indicate the H7N3 viruses with the 66-nt deletion at the neuraminidase stalk region (the NA of these 2 viruses was modified to exclude the deletion for this analysis). Both low-pathogenicity (turquoise) and HPAIV (turquoise with bolded black outline) viruses were recovered from the SC-02 premises (the hemagglutinin of the 2 HPAIVs excludes the insertion for this analysis).

H7N3 viruses from North Carolina and South Carolina was January 25, 2020 (95% Bayesian credible interval [BCI] December 14, 2019–February 28, 2020; PP = 1.0). The tMRCA, in addition to the NA stalk deletion indicating adaptation to gallinaceous poultry, potentially extends that estimate before the first detections. The estimated tMRCA of LPAIV and HPAIV from the HPAIV-positive premises was March 19, 2020 (95% BCI March 11, 2020–March 28, 2020; PP = 0.99); however, these estimates are countered by serial weekly negative diagnostic tests obtained from the same flock before onset of clinical signs. Other indicators suggestive of early detection of LPAI and mutation to HPAI include HPAIV being identified in only 1 of the 5 houses, each of the HPAIV isolates demonstrating a mixed LPAIV/HPAIV population by next-generation sequencing; active virus replication (relative cycle threshold values for each of the houses: 37, 20, 18, 23, 29) with a low level of seropositivity (only 1 detectable H7 titer [1:32] of 10 serum samples collected in the HPAIV-affected house).

Although no wild bird-origin precursor had all 8 segments that corresponded to the North Carolina and South Carolina H7N3 viruses, the most probable progenitor gene was identified for each individual segment as LPAIV originating from wild wa-

terfowl migrating along the Mississippi flyway (PP 0.92–1.00). These findings suggest that a precursor virus most likely emerged in wild waterfowl in the Mississippi flyway, with subsequent introduction into poultry via occasional virus spread between migratory flyways (11). The genomes of North American LPAIVs appear to reassort at a remarkably high rate with no apparent pattern of gene segment association (12).

Wild bird origin H7 LPAIVs have repeatedly spilled over from wild birds into poultry in North and South America, Europe, Asia, Africa, and Australia (13); on 28 recorded occasions, they have mutated into HPAIV (1). These findings highlight the importance of global surveillance in wild birds and continued vigilance in biosecurity and surveillance in worldwide poultry populations.

Acknowledgments

The authors are grateful for the diagnostic testing laboratories (the Rollins Animal Disease Diagnostic Laboratory and the Clemson Veterinary Diagnostic Center, both members of the National Animal Health Laboratory Network) and state animal health authorities in North Carolina and South Carolina, including the state veterinarians (Douglas Meckes in North Carolina and

Boyd Parr in South Carolina), as well as their respective National Poultry Improvement Program officials (Michael Martin for North Carolina and Julie Helm for South Carolina) for their rapid response and recovery efforts.

This research was supported by the United States Department of Agriculture (USDA), Agricultural Research Service (ARS) project no. 6612-32000-066-00D and by the USDA/ARS Animal and Plant Health Inspection Service (APHIS) Interagency Agreement no. 60-6040-6-005. Its contents are solely the responsibility of the authors and do not necessarily represent the official views of the USDA.

About the Author

Dr. Youk is a postdoctoral researcher at the Southeast Poultry Research Laboratory, Agricultural Research Service, US Department of Agriculture, Athens, Georgia, USA. His research interests focus on molecular epidemiology and pathobiology of avian influenza viruses.

References

1. Lee DH, Criado MF, Swayne DE. Pathobiological origins and evolutionary history of highly pathogenic avian influenza viruses. *Cold Spring Harb Perspect Med*. 2020 Jan 21 [Epub ahead of print]. <https://doi.org/10.1101/cshperspect.a038679>
2. Lee DH, Torchetti MK, Killian ML, Berhane Y, Swayne DE. Highly pathogenic avian influenza A(H7N9) virus, Tennessee, USA, March 2017. *Emerg Infect Dis*. 2017;23:1860-3. <https://doi.org/10.3201/eid2311.171013>
3. Khatchikian D, Orlich M, Rott R. Increased viral pathogenicity after insertion of a 28S ribosomal RNA sequence into the haemagglutinin gene of an influenza virus. *Nature*. 1989;340:156-7. <https://doi.org/10.1038/340156a0>
4. Maurer-Stroh S, Lee RT, Gunalan V, Eisenhaber F. The highly pathogenic H7N3 avian influenza strain from July 2012 in Mexico acquired an extended cleavage site through recombination with host 28S rRNA. *Virology*. 2013;10:139. <https://doi.org/10.1186/1743-422X-10-139>
5. Li J, Zu Dohna H, Cardona CJ, Miller J, Carpenter TE. Emergence and genetic variation of neuraminidase stalk deletions in avian influenza viruses. *PLoS One*. 2011;6:e14722. <https://doi.org/10.1371/journal.pone.0014722>
6. Stamatakis A. RAxML version 8: a tool for phylogenetic analysis and post-analysis of large phylogenies. *Bioinformatics*. 2014;30:1312-3. <https://doi.org/10.1093/bioinformatics/btu033>
7. Suchard MA, Lemey P, Baele G, Ayres DL, Drummond AJ, Rambaut A. Bayesian phylogenetic and phylodynamic data integration using BEAST 1.10. *Virus Evol*. 2018;4:vey016. <https://doi.org/10.1093/ve/vey016>
8. Youk S, Lee DH, Ferreira HL, Afonso CL, Absalon AE, Swayne DE, et al. Rapid evolution of Mexican H7N3 highly pathogenic avian influenza viruses in poultry. *PLoS One*. 2019;14:e0222457. <https://doi.org/10.1371/journal.pone.0222457>
9. Lee DH, Torchetti MK, Killian ML, Swayne DE. Deep sequencing of H7N8 avian influenza viruses from surveillance zone supports H7N8 high pathogenicity avian influenza was limited to a single outbreak farm in Indiana during 2016. *Virology*. 2017;507:216-9. <https://doi.org/10.1016/j.virol.2017.04.025>
10. Bandelt HJ, Forster P, Röhl A. Median-joining networks for inferring intraspecific phylogenies. *Mol Biol Evol*. 1999;16:37-48. <https://doi.org/10.1093/oxfordjournals.molbev.a026036>
11. Fourment M, Darling AE, Holmes EC. The impact of migratory flyways on the spread of avian influenza virus in North America. *BMC Evol Biol*. 2017;17:118. <https://doi.org/10.1186/s12862-017-0965-4>
12. Dugan VG, Chen R, Spiro DJ, Sengamalay N, Zaborsky J, Ghedin E, et al. The evolutionary genetics and emergence of avian influenza viruses in wild birds. *PLoS Pathog*. 2008;4:e1000076. <https://doi.org/10.1371/journal.ppat.1000076>
13. World Organization for Animal Health. World Animal Health Information Database Interface: disease information [cited 2020 May 5]. https://www.oie.int/wahis_2/public/wahid.php/Diseaseinformation/Immsummary

Address for correspondence: Dong-Hun Lee, University of Connecticut, 61 N Eagleville Rd, Storrs, CT 06269 USA; email: dong-hun.lee@uconn.edu

Highly Pathogenic Avian Influenza A(H7N3) Virus in Poultry, United States, 2020

Appendix

Materials and Methods

Virus Sampling and Sequencing

The initial detections were made through routine and active surveillance testing, and the enhanced surveillance of the affected and epidemiologically related premises followed. All the turkey farms that tested positive for low pathogenic avian influenza (LPAI) H7N3 recorded clinical signs related to avian influenza infection such as slight drops in egg production and mild respiratory signs. During the surveillance, influenza H7 was detected in another commercial turkey flock in South Carolina that reported an increased daily mortality (4.6%). Two samples from a single house at these premises was confirmed positive for highly pathogenic avian influenza (HPAI) H7N3 by sequencing; the other 4 houses in the same farm were confirmed positive for LPAI H7N3. In March and April, >3,700 pooled swabs from oropharynx and cloaca were tested, representing nearly 19,000 birds. Of those, 48 (1.3%) pooled samples from 13 premises tested positive for influenza A and 44 (1.2%) tested positive for H7 by gene PCR (1,2). A total of 29 H7N3 viruses were amplified by RT-PCR (3) and sequenced using the Ion Torrent Personal Genome Machine (Life Technologies, <https://www.thermofisher.com>) and/or MiSeq (Illumina, <https://www.illumina.com>) platforms, as previously described (4). De novo and directed assembly of genome sequences were carried out using the SeqMan NGen v. Four program. Nucleotide sequences for complete genomes of H7N3 viruses have been deposited in GenBank under accession nos. MT444183–MT444350 and MT444352–MT444415.

Phylogenetic Analysis

Genome sequences of wild bird avian influenza viruses (AIVs) close to the initial H7N3 viruses in turkeys were examined by BLAST function (<https://blast.ncbi.nlm.nih.gov>, accessed March 2020; 100 outputs), and added to the NC and SC H7N3 viruses analysis for each gene

segment. Alignment of the complete genome sequences was performed using MAFFT (<http://mafft.cbrc.jp/alignment/software>). Maximum-likelihood (ML) phylogeny of each gene segment was generated by using RAxML (5). Bootstrap support values were generated using 1,000 rapid replicates.

To estimate viral gene transition and demographic history of each segment, we inferred time-scaled phylogenies by Bayesian Markov chain Monte Carlo (MCMC) sampling using BEAST v1.10.4 (<https://www.mybiosoftware.com>). From the ML phylogenetic analysis, potential outliers that considerably deviated from the root-to-tip distance against time were removed from this study by using TempEst v1.5.1 (6). To trace the most probable ancestral wild bird viruses that generated the North Carolina and South Carolina H7N3 viruses, a discrete state ancestral reconstruction approach was implemented using bird flyways as discrete ancestral character states, including the Atlantic, Mississippi, Central, and Pacific flyways. We used an uncorrelated lognormal distribution relaxed clock method, the HKY nucleotide substitution model, and the GMRF Bayesian skyride coalescent prior (7). An asymmetric substitution model with the Bayesian stochastic search variable selection and a strict clock model were used for the discrete nominal category. At least 3 independent Markov chains were performed to meet the basis of the criterion of an effective sampling size of >200 as calculated by Tracer version 1.5 with a 10% burn-in (<http://tree.bio.ed.ac.uk/software/tracer>). Maximum clade credibility trees were generated for each gene segment by using TreeAnnotator (<http://www.phylo.org/index.php/tools/treeannotator.html>) and were visualized using FigTree 1.4.4 (<http://tree.bio.ed.ac.uk>).

To increase phylogenetic resolution, nucleotide sequences of the entire protein coding regions of each virus were concatenated with modified hemagglutinin (HA) and neuraminidase (NA) gene sequences to exclude the insertion at the HA cleavage site and the deletion at the NA stalk region, and then analyzed with Bayesian and median-joining (MJ) network phylogenetic analysis (8,9). Based on marginal likelihoods of various demographic models estimated by path sampling and stepping-stone analysis, we chose the relaxed clock model, the HKY nucleotide substitution model, and coalescent exponential population prior for a Bayesian framework (10). At least 3 independent Markov chains were performed to meet the basis of the criterion of an effective sampling size of >200 as calculated by Tracer version 1.5 with a 10% burn-in.

Maximum clade credibility trees were generated for each gene segment by using TreeAnnotator and were visualized by using FigTree 1.4.4.

Pathotyping Test

The intravenous pathogenicity index (IVPI) test was conducted in chickens according to the OIE Manual of Diagnostic Tests and Vaccines for Terrestrial Animals (<http://www.oie.int/en/international-standard-setting/terrestrial-manual>). In brief, 0.1 mL of infectious allantoic fluid was inoculated intravenously into 10 6-week-old specific-pathogen-free chickens and the chickens were monitored for 10 days for illness and death. Isolates with IVPI >1.2 were characterized as HPAIV. The challenge studies and all experiments with live viruses were conducted in a biosafety level 3 facility at the National Veterinary Services Laboratories, Animal and Plant Health Inspection Service, US Department of Agriculture in Ames, Iowa, USA, in accordance with approved institutional animal care and use protocols.

References

1. Spackman E. Avian influenza virus detection and quantitation by real-time RT-PCR. *Methods Mol Biol.* 2020;2123:137–48. [PubMed https://doi.org/10.1007/978-1-0716-0346-8_11](https://doi.org/10.1007/978-1-0716-0346-8_11)
2. Spackman E, Senne DA, Myers TJ, Bulaga LL, Garber LP, Perdue ML, et al. Development of a real-time reverse transcriptase PCR assay for type A influenza virus and the avian H5 and H7 hemagglutinin subtypes. *J Clin Microbiol.* 2002;40:3256–60. [PubMed https://doi.org/10.1128/jcm.40.9.3256-3260.2002](https://doi.org/10.1128/jcm.40.9.3256-3260.2002)
3. Lee DH. Complete genome sequencing of influenza A viruses using next-generation sequencing. *Methods Mol Biol.* 2020;2123:69–79. [PubMed https://doi.org/10.1007/978-1-0716-0346-8_6](https://doi.org/10.1007/978-1-0716-0346-8_6)
4. Lee DH, Torchetti MK, Killian ML, Swayne DE. Deep sequencing of H7N8 avian influenza viruses from surveillance zone supports H7N8 high pathogenicity avian influenza was limited to a single outbreak farm in Indiana during 2016. *Virology.* 2017;507:216–9. [PubMed https://doi.org/10.1016/j.virol.2017.04.025](https://doi.org/10.1016/j.virol.2017.04.025)
5. Stamatakis A. RAxML version 8: a tool for phylogenetic analysis and post-analysis of large phylogenies. *Bioinformatics.* 2014;30:1312–3. [PubMed https://doi.org/10.1093/bioinformatics/btu033](https://doi.org/10.1093/bioinformatics/btu033)

6. Rambaut A, Lam TT, Max Carvalho L, Pybus OG. Exploring the temporal structure of heterochronous sequences using TempEst (formerly Path-O-Gen). *Virus Evol.* 2016;2:vew007.
<https://doi.org/10.1093/ve/vew007>
7. Minin VN, Bloomquist EW, Suchard MA. Smooth skyride through a rough skyline: Bayesian coalescent-based inference of population dynamics. *Mol Biol Evol.* 2008;25:1459–71. [PubMed](#)
<https://doi.org/10.1093/molbev/msn090>
8. Bandelt HJ, Forster P, Röhl A. Median-joining networks for inferring intraspecific phylogenies. *Mol Biol Evol.* 1999;16:37–48. [PubMed](#) <https://doi.org/10.1093/oxfordjournals.molbev.a026036>
9. Suchard MA, Lemey P, Baele G, Ayres DL, Drummond AJ, Rambaut A. Bayesian phylogenetic and phylodynamic data integration using BEAST 1.10. *Virus Evol.* 2018;4:vey016.
<https://doi.org/10.1093/ve/vey016>
10. Baele G, Li WL, Drummond AJ, Suchard MA, Lemey P. Accurate model selection of relaxed molecular clocks in Bayesian phylogenetics. *Mol Biol Evol.* 2013;30:239–43. [PubMed](#)
<https://doi.org/10.1093/molbev/mss243>

Appendix Table 1. Avian influenza H7N3 viruses isolated and sequenced in this study*

Date collected	Virus strain	Premises	Operation type	Changes in HA cleavage site	Changes in NA stalk region	IVPI
2020 Mar 9	A/turkey/North_Carolina/20-007949-001/2020(H7N3)	NC-01	Commercial, breeder	N/A	N/A	0
2020 Mar 9	A/turkey/North_Carolina/20-007949-002/2020(H7N3)	NC-01	Commercial, breeder	N/A	N/A	ND
2020 Mar 10	A/turkey/North_Carolina/20-007948-002/2020(H7N3)	NC-04	Commercial, meat-type	N/A	N/A	ND
2020 Mar 10	A/turkey/North_Carolina/20-007948-003/2020(H7N3)	NC-04	Commercial, meat-type	N/A	N/A	ND
2020 Mar 10	A/turkey/North_Carolina/20-007948-005/2020(H7N3)	NC-04	Commercial, meat-type	N/A	N/A	ND
2020 Mar 12	A/turkey/North_Carolina/20-008256-001/2020(H7N3)	NC-01	Commercial, breeder	N/A	N/A	ND
2020 Mar 12	A/turkey/North_Carolina/20-008256-002/2020(H7N3)	NC-01	Commercial, breeder	N/A	N/A	ND
2020 Mar 12	A/turkey/North_Carolina/20-008257-001/2020(H7N3)	NC-03	Commercial, meat-type	Single basic amino acid substitution	N/A	0
2020 Mar 12	A/turkey/North_Carolina/20-008257-002/2020(H7N3)	NC-03	Commercial, meat-type	Single basic amino acid substitution	N/A	ND
2020 Mar 12	A/turkey/North_Carolina/20-008258-001/2020(H7N3)	NC-04	Commercial, meat-type	N/A	N/A	ND
2020 Mar 12	A/turkey/North_Carolina/20-008258-002/2020(H7N3)	NC-04	Commercial, meat-type	N/A	N/A	ND
2020 Mar 13	A/turkey/North_Carolina/20-008395-002/2020(H7N3)	NC-02	Commercial, meat-type	Single basic amino acid substitution	N/A	ND
2020 Mar 13	A/turkey/North_Carolina/20-008395-003/2020(H7N3)	NC-02	Commercial, meat-type	Single basic amino acid substitution	N/A	ND
2020 Mar 13	A/turkey/North_Carolina/20-008423-002/2020(H7N3)	NC-05	Commercial, meat-type	N/A	66 nt deletion	ND
2020 Mar 13	A/turkey/North_Carolina/20-008425-001/2020(H7N3)	NC-06	Commercial, meat-type	N/A	66 nt deletion	0
2020 Mar 13	A/turkey/South_Carolina/20-008394-001/2020(H7N3)	SC-01	Commercial, meat-type	N/A	N/A	0
2020 Mar 15	A/turkey/North_Carolina/20-008421-001/2020(H7N3)	NC-07	Commercial, meat-type	N/A	N/A	ND
2020 Mar 17	A/turkey/North_Carolina/20-008734-001/2020(H7N3)	NC-07	Commercial, breeder	N/A	N/A	ND
2020 Mar 19	A/turkey/North_Carolina/20-009000-001/2020(H7N3)	NC-08	Commercial, meat-type	N/A	N/A	ND
2020 Mar 19	A/turkey/North_Carolina/20-009000-002/2020(H7N3)	NC-08	Commercial, meat-type	N/A	N/A	ND
2020 Mar 19	A/turkey/North_Carolina/20-009000-004/2020(H7N3)	NC-08	Commercial, meat-type	N/A	N/A	ND
2020 Mar 30	A/turkey/North_Carolina/20-010036-002/2020(H7N3)	NC-09	Commercial, meat-type	N/A	N/A	ND
2020 Mar 30	A/turkey/North_Carolina/20-010036-004/2020(H7N3)	NC-09	Commercial, meat-type	N/A	N/A	ND
2020 Mar 30	A/turkey/North_Carolina/20-010036-005/2020(H7N3)	NC-09	Commercial, meat-type	N/A	N/A	ND
2020 Apr 6	A/turkey/South_Carolina/20-010561-002/2020(H7N3)	SC-02	Commercial, meat-type	N/A	N/A	0
2020 Apr 6	A/turkey/South_Carolina/20-010561-003/2020(H7N3)	SC-02	Commercial, meat-type	27 nt insertion	N/A	ND
2020 Apr 6	A/turkey/South_Carolina/20-010561-004/2020(H7N3)	SC-02	Commercial, meat-type	N/A	N/A	ND
2020 Apr 6	A/turkey/South_Carolina/20-010561-005/2020(H7N3)	SC-02	Commercial, meat-type	N/A	N/A	ND
2020 Apr 6	A/turkey/South_Carolina/20-010561-006/2020(H7N3)	SC-02	Commercial, meat-type	27 nt insertion	N/A	2.47

*HA, hemagglutinin; IVPI, intravenous pathogenicity index; NA, neuraminidase; N/A, not applicable; ND, not done.

Appendix Table 2. Mammalian host-specific genetic markers*

Strain	Segment and amino acid change															
	HA		PB2			PB1		PA		NP			NS1			
	Q226L	G228S	Q591K	E627K	D701N	K353R	T566A	S409N	K615N	R99K	N319K	S345N	S42P	D92E	F103L	M106I
A/turkey/North_Carolina/20-007948-002/2020	Q	G	Q	E	D	K	T	S	K	R	N	S	S	D	F	M
A/turkey/North_Carolina/20-007948-003/2020	Q	G	Q	E	D	K	T	S	K	R	N	S	S	D	F	M
A/turkey/North_Carolina/20-007948-005/2020	Q	G	Q	E	D	K	T	S	K	R	N	S	S	D	F	M
A/turkey/North_Carolina/20-007949-001/2020	Q	G	Q	E	D	K	T	S	K	R	N	S	S	D	F	M
A/turkey/North_Carolina/20-007949-002/2020	Q	G	Q	E	D	K	T	S	K	R	N	S	S	D	F	M
A/turkey/North_Carolina/20-008256-001/2020	Q	G	Q	E	D	K	T	S	K	R	N	S	S	D	F	M
A/turkey/North_Carolina/20-008256-002/2020	Q	G	Q	E	D	K	T	S	K	R	N	S	S	D	F	M
A/turkey/North_Carolina/20-008257-001/2020	Q	G	Q	E	D	K	T	S	K	R	N	S	S	D	F	M
A/turkey/North_Carolina/20-008257-002/2020	Q	G	Q	E	D	K	T	S	K	R	N	S	S	D	F	M
A/turkey/North_Carolina/20-008258-001/2020	Q	G	Q	E	D	K	T	S	K	R	N	S	S	D	F	M
A/turkey/North_Carolina/20-008258-002/2020	Q	G	Q	E	D	K	T	S	K	R	N	S	S	D	F	M
A/turkey/North_Carolina/20-008395-002/2020	Q	G	Q	E	D	K	T	S	K	R	N	S	S	D	F	M
A/turkey/North_Carolina/20-008395-003/2020	Q	G	Q	E	D	K	T	S	K	R	N	S	S	D	F	M
A/turkey/North_Carolina/20-008421-001/2020	Q	G	Q	E	D	K	T	S	K	R	N	S	S	D	F	M
A/turkey/North_Carolina/20-008423-002/2020	Q	G	Q	E	D	K	T	S	K	R	N	S	S	D	F	M
A/turkey/North_Carolina/20-008425-001/2020	Q	G	Q	E	D	K	T	S	K	R	N	S	S	D	F	M
A/turkey/North_Carolina/20-008734-001/2020	Q	G	Q	E	D	K	T	S	K	R	N	S	S	D	F	M
A/turkey/North_Carolina/20-009000-001/2020	Q	G	Q	E	D	K	T	S	K	R	N	S	S	D	F	M
A/turkey/North_Carolina/20-009000-002/2020	Q	G	Q	E	D	K	T	S	K	R	N	S	S	D	F	M
A/turkey/North_Carolina/20-009000-004/2020	Q	G	Q	E	D	K	T	S	K	R	N	S	S	D	F	M
A/turkey/North_Carolina/20-010036-002/2020	Q	G	Q	E	D	K	T	S	K	R	N	S	S	D	F	M
A/turkey/North_Carolina/20-010036-004/2020	Q	G	Q	E	D	K	T	S	K	R	N	S	S	D	F	M
A/turkey/North_Carolina/20-010036-005/2020	Q	G	Q	E	D	K	T	S	K	R	N	S	S	D	F	M

Strain	Segment and amino acid change															
	HA		PB2			PB1		PA		NP			NS1			
	Q226L	G228S	Q591K	E627K	D701N	K353R	T566A	S409N	K615N	R99K	N319K	S345N	S42P	D92E	F103L	M106I
A/turkey/South_Carolina/20-008394-001/2020	Q	G	Q	E	D	K	T	S	K	R	N	S	S	D	F	M
A/turkey/South_Carolina/20-010561-002/2020	Q	G	Q	E	D	K	T	S	K	R	N	S	S	D	F	M
A/turkey/South_Carolina/20-010561-003/2020	Q	G	Q	E	D	K	T	S	K	R	N	S	S	D	F	M
A/turkey/South_Carolina/20-010561-004/2020	Q	G	Q	E	D	K	T	S	K	R	N	S	S	D	F	M
A/turkey/South_Carolina/20-010561-005/2020	Q	G	Q	E	D	K	T	S	K	R	N	S	S	D	F	M
A/turkey/South_Carolina/20-010561-006/2020	Q	G	Q	E	D	K	T	S	K	R	N	S	S	D	F	M

* D, aspartic acid; E, glutamic acid; F, phenylalanine; G, glycine; HA, hemagglutinin; K, lysine; M, methionine; N, asparagine; NP, nucleoprotein; NS, nonstructural protein; PA, polymerase; PB, polymerase basic; Q, glutamine; R, arginine; S, serine; T, threonine.

D



NC and SC H7N9

Tennessee H7N9

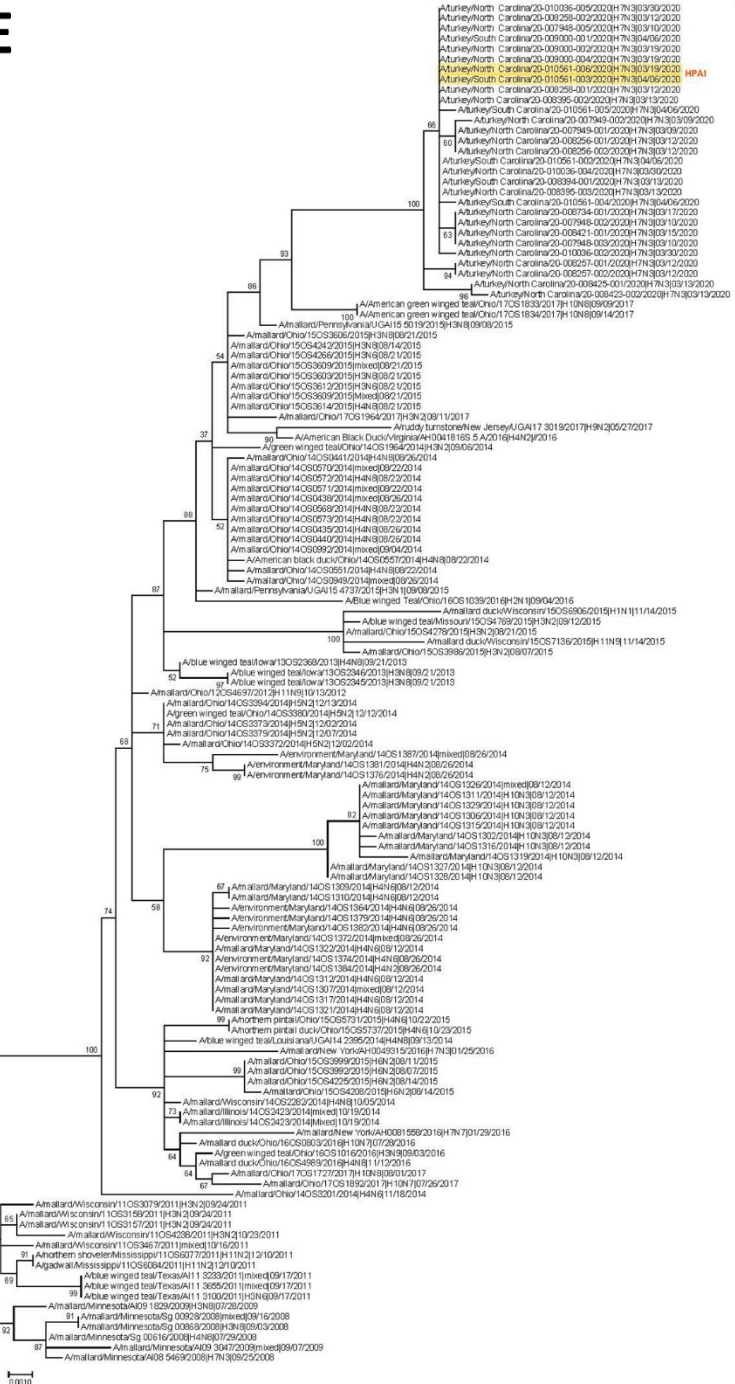
Indiana H7N9

Mexico H7N9

China H7N9

0.050

E



NC and SC H7N9

F



NC and SC H7N3

MP AI

Mexico H7N3

G





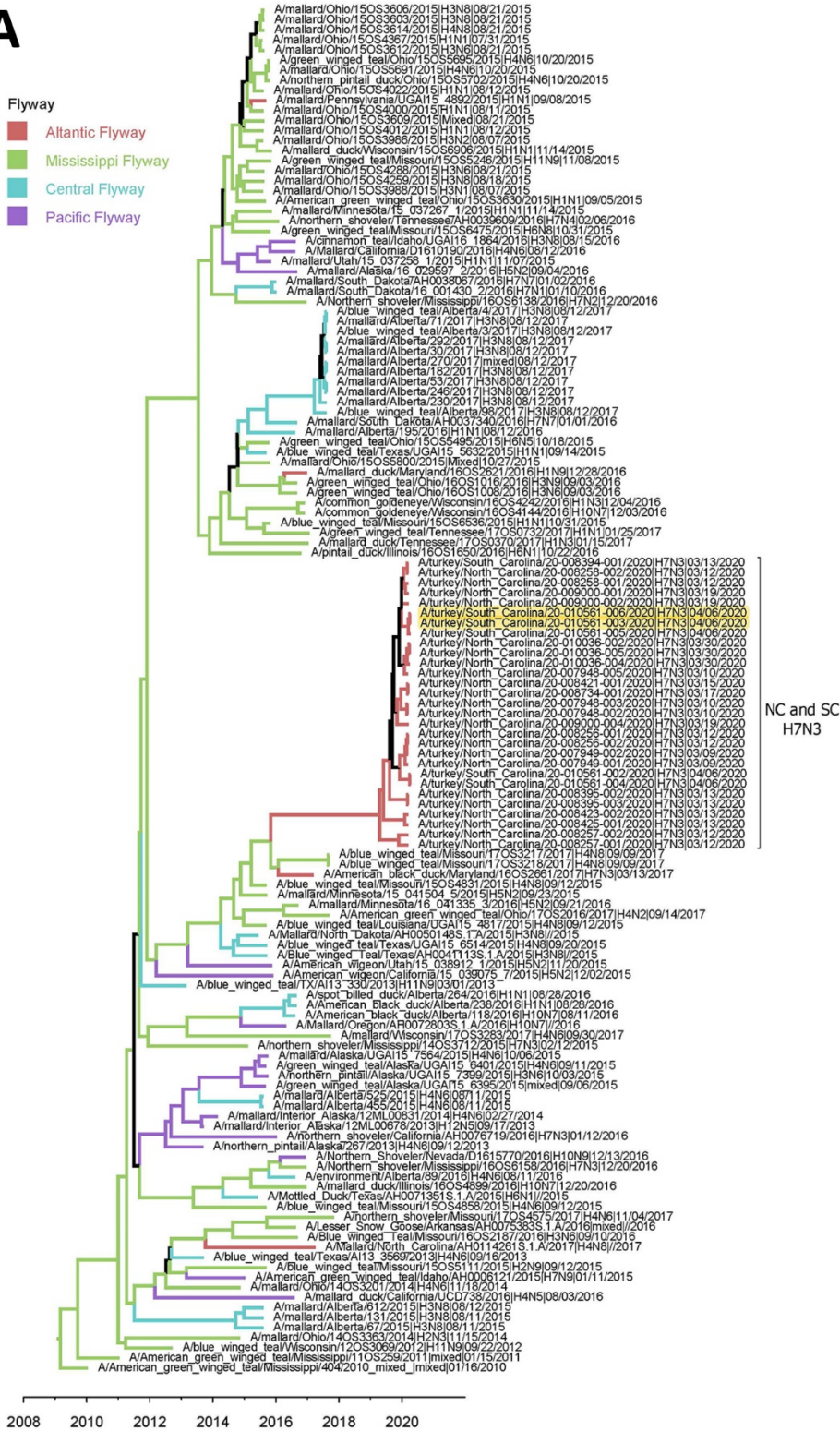
NC and SC H7N3

Appendix Figure 1. Maximum likelihood trees with ancestral wild bird avian influenza viruses. At each branch, the number indicates a bootstrap value. A) polymerase basic 2 (PB2); B) PB1; C) polymerase (PA); D) hemagglutinin (HA); E) nucleoprotein (NP); F) neuraminidase (NA); G) matrix (M); H) nonstructural (NS).

A

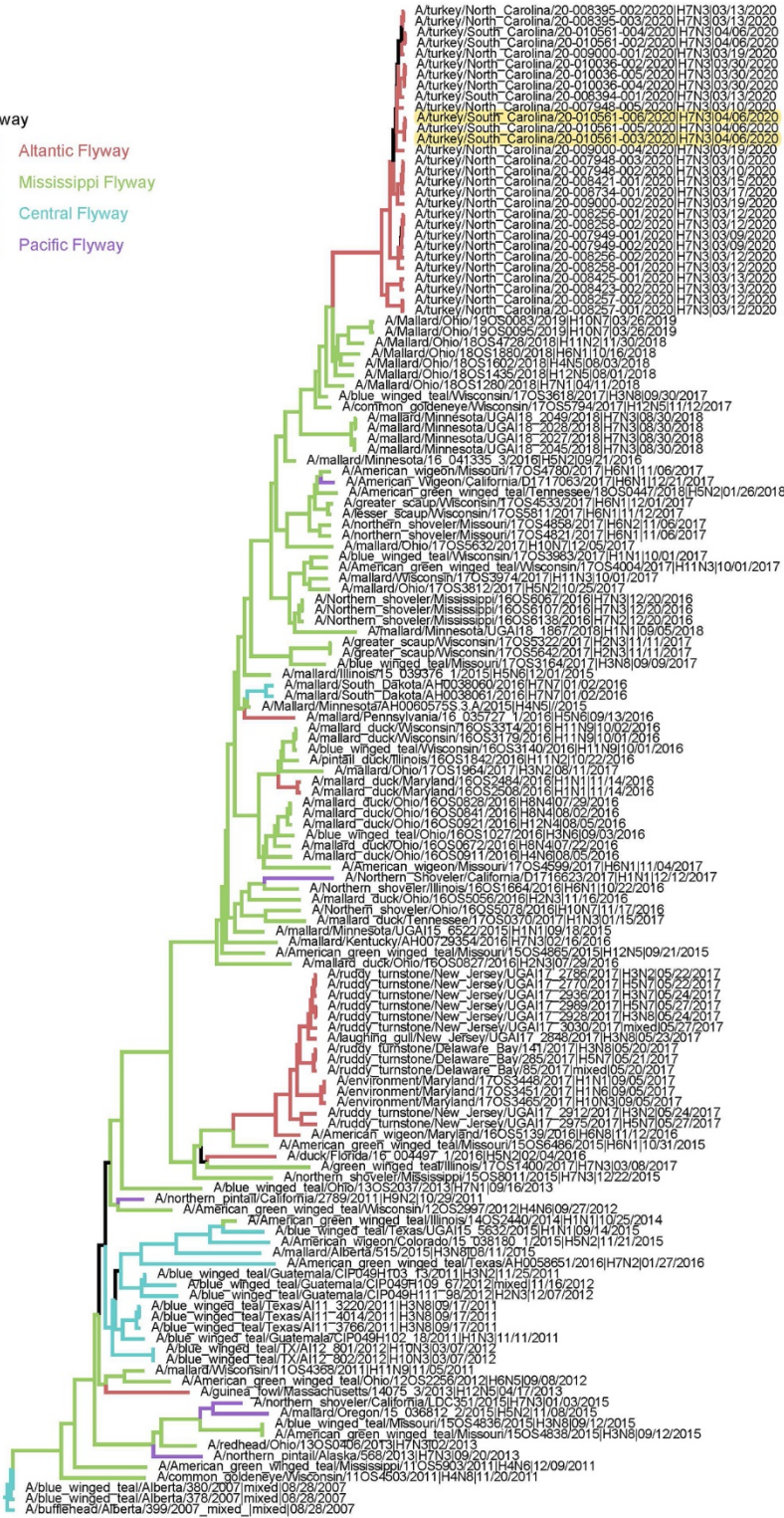
Flyway

- Atlantic Flyway
- Mississippi Flyway
- Central Flyway
- Pacific Flyway



C

- Flyway
- Atlantic Flyway
 - Mississippi Flyway
 - Central Flyway
 - Pacific Flyway



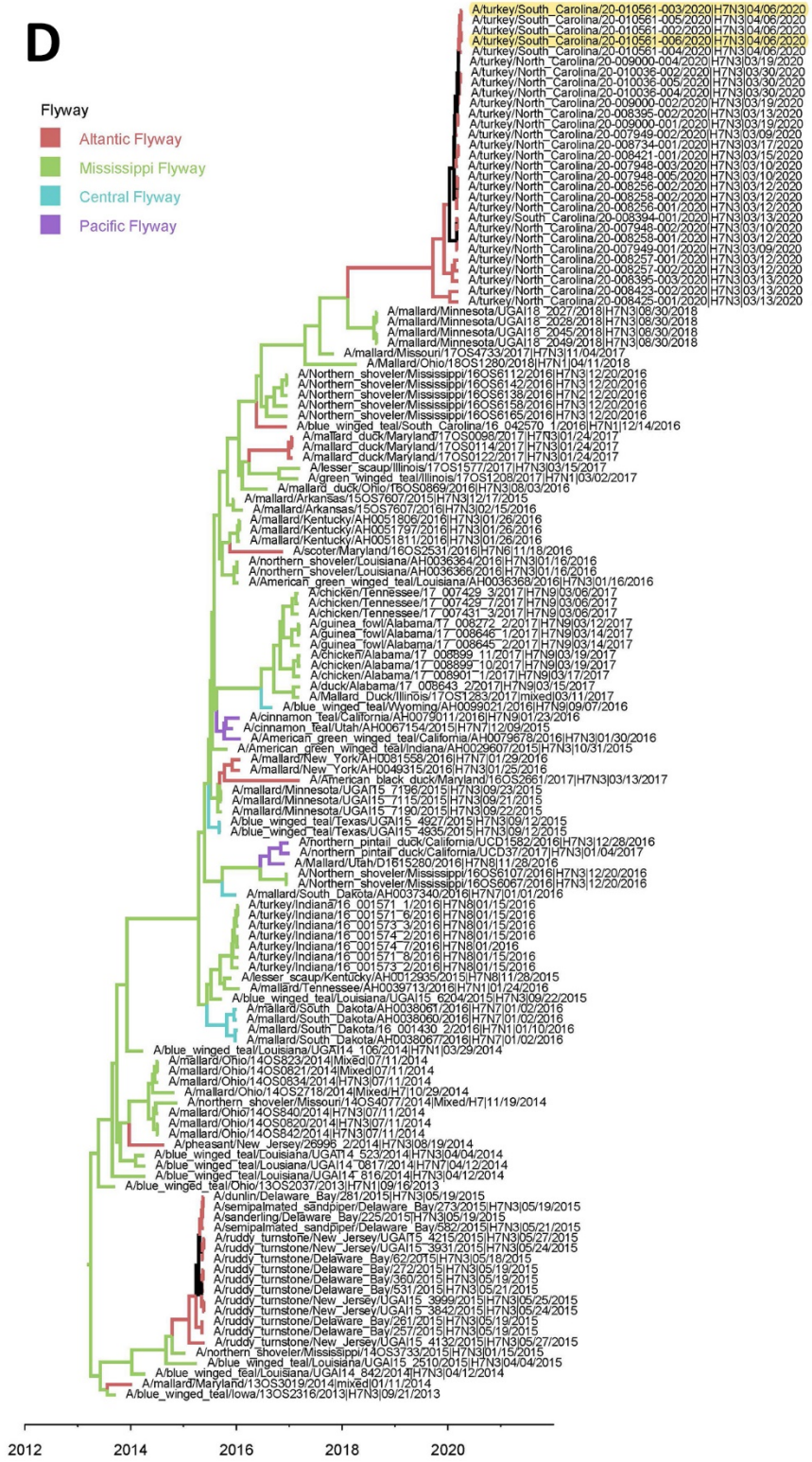
NC and SC
H7N3

2006 2008 2010 2012 2014 2016 2018 2020 2022

D

Flyway

- Altantic Flyway
- Mississippi Flyway
- Central Flyway
- Pacific Flyway

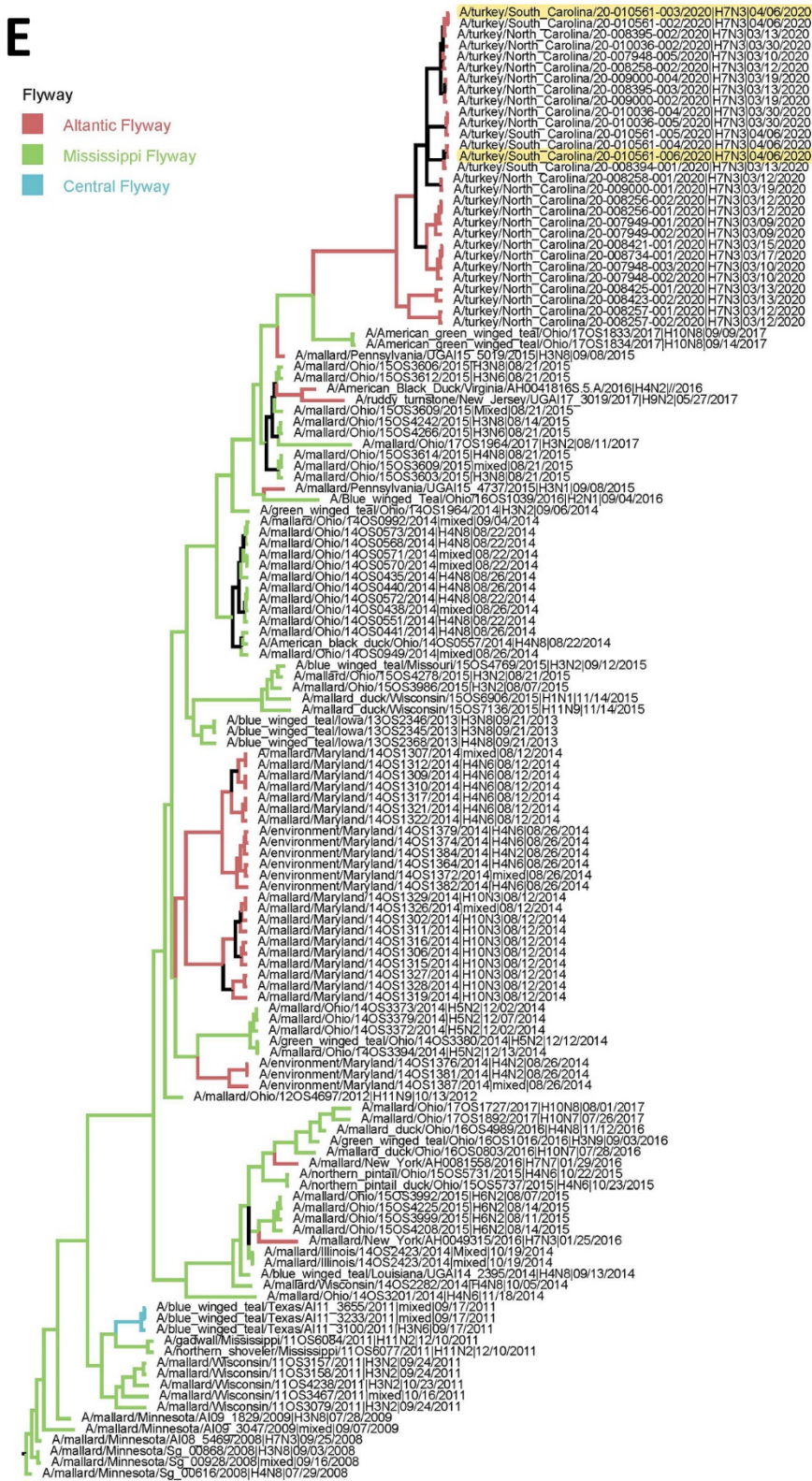


NC and SC
H7N3

E

Flyway

- Atlantic Flyway
- Mississippi Flyway
- Central Flyway



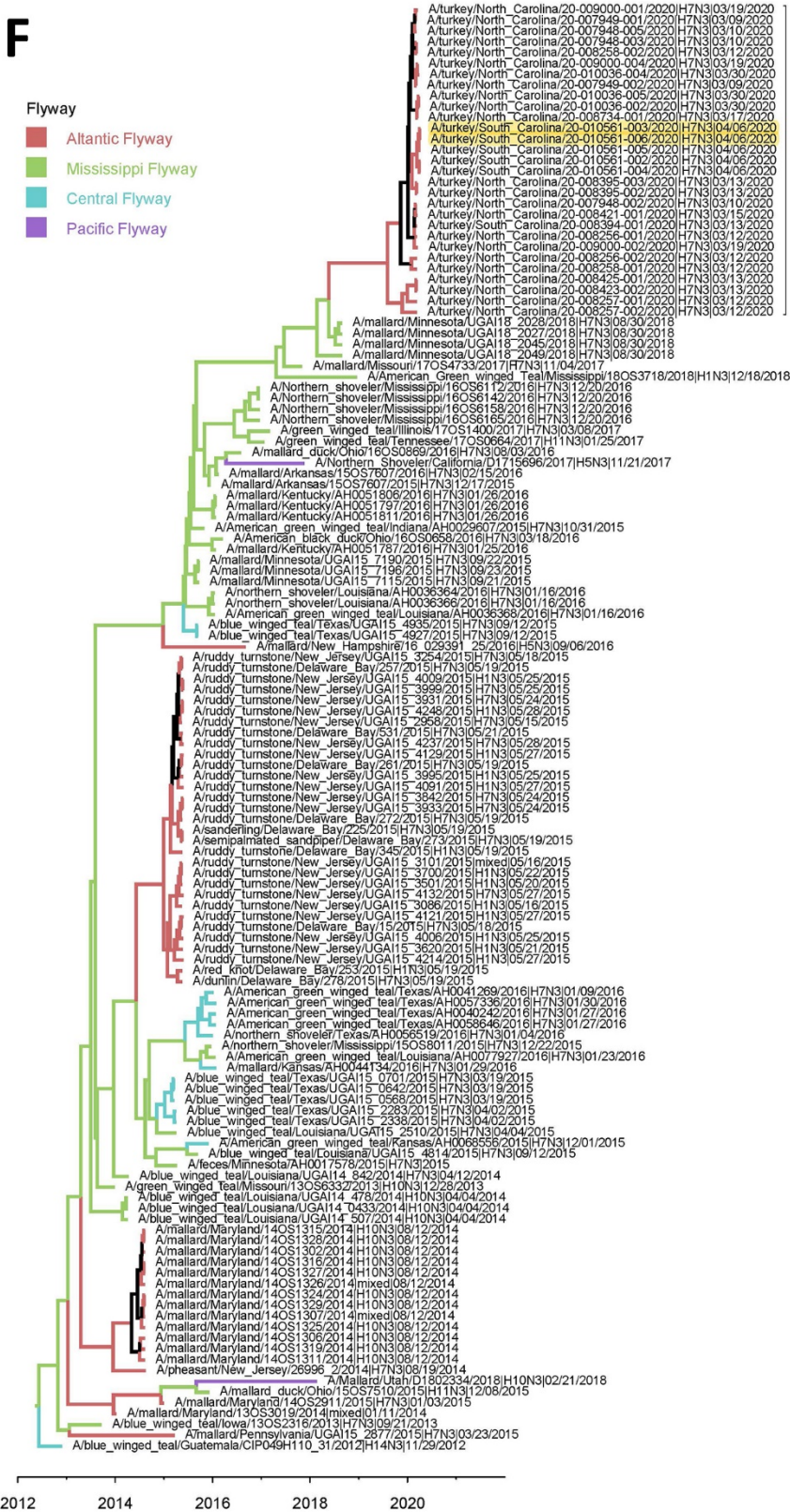
NC and SC
H7N3

2008 2010 2012 2014 2016 2018 2020

F

Flyway

- Atlantic Flyway
- Mississippi Flyway
- Central Flyway
- Pacific Flyway

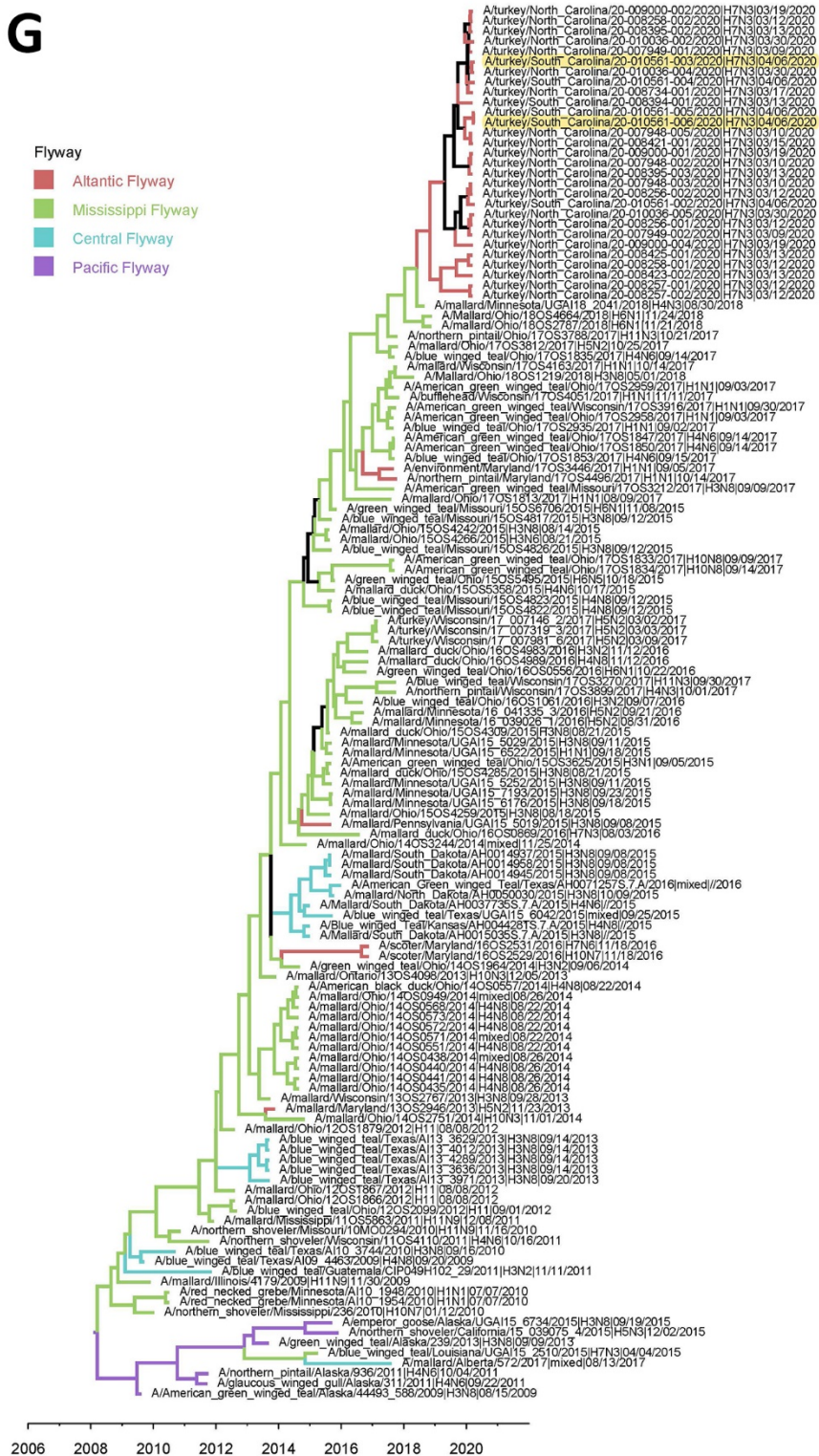


NC and SC
H7N3

G

Flyway

- Atlantic Flyway
- Mississippi Flyway
- Central Flyway
- Pacific Flyway

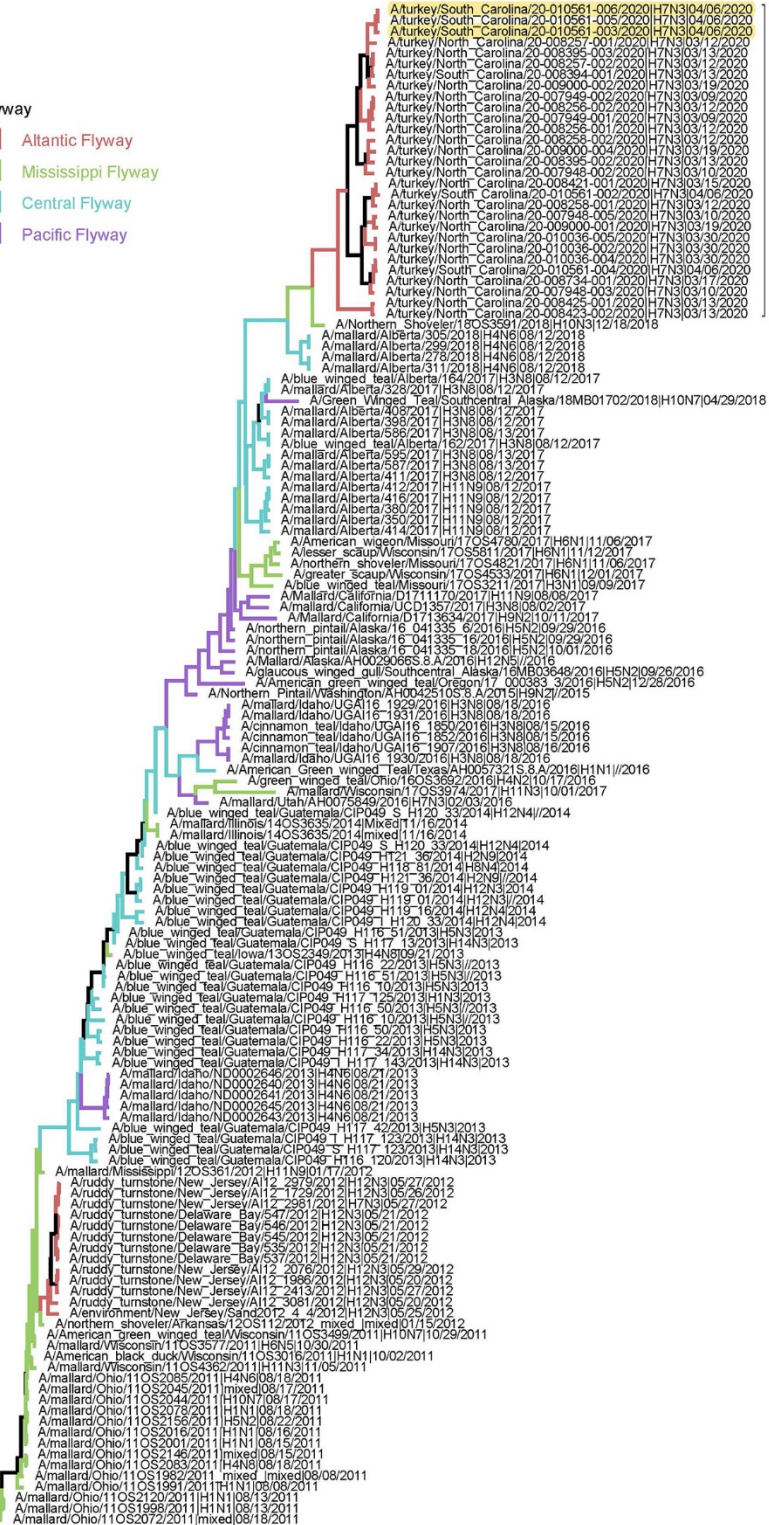


NC and SC
H7N3

H

Flyway

- Atlantic Flyway
- Mississippi Flyway
- Central Flyway
- Pacific Flyway



NC and SC
H7N3

Appendix Figure 2. Time-scaled Bayesian phylogenetic trees. Branches are colored according to discrete geographic areas including 4 administrative bird flyways in North America (Atlantic, Mississippi,

Central, and Pacific) according to the flyway boundaries established by the US Fish and Wildlife Service. Blue node bars represent 95% Bayesian credible intervals (BCI). A) polymerase basic 2 (PB2); B) PB1; C) polymerase (PA); D) hemagglutinin (HA); E) nucleoprotein (NP); F) neuraminidase (NA); G) matrix (M); H) nonstructural (NS).